JOURNAL OF CATALYSIS 94, 385–399 (1985)

Studies of Carbon- and Hydrogen-Containing Adspecies Present during CO Hydrogenation over Unsupported Ru, Ni, and Rh

PHILIP WINSLOW AND ALEXIS T. BELL

Materials and Molecular Research Division, Lawrence Berkeley Laboratory; and Department of Chemical Engineering, University of California, Berkeley, California 94720

Received August 20, 1984; revised March 20, 1985

Isotopic tracer studies have been conducted to determine the coverages of adsorbed CO, carbon, and hydrogen on the surfaces of unsupported Ru, Rh, and Ni powders during CO hydrogenation. Two forms of hydrogen are observed on each catalyst at 298 K: a low-energy form which is in equilibrium with the gas phase and is rapidly displaced from the surface by CO adsorption and a high-energy form which is not in equilibrium with the gas phase and is not displaced by CO adsorption. The low-energy form is ascribed to hydrogen adsorbed on the exterior surfaces of the metal powder. It is proposed that the high-energy form may be hydrogen which has migrated along crystal grain boundaries into the interior of the metal powder. Adsorbed carbon and CO are also observed on each catalyst. It is demonstrated that high methanation activity correlates with the surface coverage of active carbon but not with the coverage of adsorbed hydrogen.

INTRODUCTION

Isotopic tracer and transient response techniques have been used effectively to characterize the surface coverages of carbon and CO present on Fe, Ni, Ru, and Rh catalysts during CO disproportionation (*1–3*) and CO hydrogenation (*2, 4–9*). These studies have revealed that multiple forms of carbon can coexist in the presence of adsorbed CO. Nascent carbon formed by the disproportionation of CO is very active. This carbon is readily converted to methane with H_2 (*1*) as well as methane and other hydrocarbons in the presence of H_2 and CO (*2, 3*).

The dynamics of incorporation of ^{13}C-labeled carbon into hydrocarbon products upon switching from a feed mixture containing H_2 and ^{12}CO to one containing H_2 and ^{13}CO yields information on the quantity and activity of adsorbed carbon species (*2, 4–6*). Additional information is obtained by observing the transient formation of hydrocarbons during the reaction of the adsorbed carbon-containing species with hydrogen (*4–9*). The resulting transients indicate the quantities of different carbon species present. Recent studies carried out with Ru/SiO_2 and Ru powder have demonstrated that methane and C_2 hydrocarbons are formed from highly active carbon species and that the rate of methane formation is directly proportional to the surface concentration of active carbon (*5, 6*). Transient response studies have also shown that a "less active" carbon accumulates on the catalyst during CO hydrogenation (*5, 7–10*). In some studies, isotopic tracer and transient response techniques have been complemented by the use of Mössbauer (*9*) and ^{13}C NMR (*11*) spectroscopy.

Much less is known about the forms and concentrations of adsorbed hydrogen present during CO hydrogenation. Attempts to measure the amount of hydrogen adsorbed on Fe/Al_2O_3 via H_2–D_2 exchange have been unsuccessful due to interference from hydroxyl groups on the support (*8*). The amount of hydrogen associated with adsorbed carbon could be determined, though, by oxygen titration. A stoichiome-

0021-9517/85 $3.00

try of $CH_{0.17}$ was obtained by this means (*8*).

The adsorption of H_2 in the presence of CO at temperatures below which reaction occurs has been investigated. Coadsorption of H_2 and CO on a supported Ni catalyst enhances the amount of H_2 adsorbed over that occurring is the absence of CO (*12*). At 348 K the stoichiometry is $H_s : CO_s : CO_2 : Ni_s = 2:1:1$. Similar stoichiometric ratios were observed for H_2 and CO coadsorption on Ru powder (*13*). Enhancement of H_2 adsorption by CO coadsorption was also noted on Rh and Ir powders, but a similar effect was not observed on Pt. The enhanced adsorption of H_2 was attributed to the formation of enolic complexes, though no spectroscopic evidence was presented to confirm these structures.

Recently, H_2–D_2 isotope tracing has been successfully applied to characterize the adsorption of H_2 in the presence of CO on unsupported Ru powder (*6*). Two forms of adsorbed hydrogen were observed. One form is atomically adsorbed on the metal surface. Surprisingly, about 0.8 monolayer equivalents of this species was observed in the presence of nearly a monolayer of CO. This is twice as much as has been estimated to be present on the surface of a Ru/SiO_2 catalyst (*14*). The second form of hydrogen on Ru powder accumulates with increasing length of CO hydrogenation (*6*). This form of hydrogen is associated with the "less active" form of carbon, such that the H/C ratio is about 2.

In this paper we present additional results for Ru powder and new data concerning the surface concentrations of adsorbed hydrogen, carbon monoxide, and carbon on Rh and Ni powders. The relationship of these measurements to the kinetics of CO hydrogenation is discussed.

EXPERIMENTAL

Experiments were carried out with a small glass reactor heated in a fluidized sand bath. Gas for the reactor was supplied from a manifold made up of two equivalent branches. The two branches connect to a low dead-volume valve which is used to select the feed stream delivered to the reactor. The reaction products were analyzed on line with a mass spectrometer connected to a microcomputer-based data acquisition system. Further details concerning the experimental apparatus are given in Refs. (*4, 5*).

Three metal powders were studied, ruthenium, rhodium, and nickel. The ruthenium powder (99.9%) was purchased from MacKay A.D., Inc., the rhodium (99.99%) from Aldrich, and the nickel (99.999%) from Alfa Chemicals.

The amount of each catalyst used for reaction studies was limited from 50 to 200 mg to minimize the pressure drop across the reactor. However, because of the small weight of catalyst, it was impossible to determine surface areas from volumetric chemisorption measurements. As a result, the surface area of each sample was measured *in situ* by D_2/H_2 displacement. A reduced sample was exposed to flowing D_2 at 298 K for 300 s and then flushed with Ar for 300 s to desorb physically adsorbed species. The sample was exposed next to flowing H_2 at 298 K to displace adsorbed deuterium in the form of HD or D_2. This step displaced only a portion of the originally chemisorbed deuterium. Additional adsorbed deuterium was displaced by ramping the temperature to 523 K, resulting in the formation of additional HD. The total amount of deuterium detected as HD or D_2 in this sequence was used to estimate the total number of surface metal atoms in the sample assuming an adsorption stoichiometry of $D_s : M_s = 1:1$ (*15, 16*). Metal powder dispersions and surface areas are given in Table 1. It is evident that all of the catalysts have extremely low dispersions.

H_2, D_2, Ar, and ^{12}CO were purified using techniques described in Ref. (*5*). ^{13}CO (83%—$^{13}C^{16}O$, 17%—$^{13}C^{18}O$) was obtained from Liquid Carbonic and used without further purification.

TABLE 1

Dispersions and Surface Areas of Ru, Rh, and Ni Powders

Metal	Dispersion[a] (%)	Surface area[a] (m^2/g)
Ru	0.17	0.62
Rh	0.12	0.54
Ni	0.016	0.11

[a] Based on H_2–D_2 displacement at 298 K. Samples flushed for 300 s in Ar to remove physisorbed species.

RESULTS

Adsorbed Hydrogen Species

Experiments were initiated by reducing the catalyst in D_2 for several hours at 523 K. The catalyst was then cooled to the desired temperature and allowed to reach equilibrium with the applied D_2 partial pressure for 1800 s. After flushing the reactor for 15 s with Ar, a stream of H_2 was introduced, resulting in the displacement of adsorbed deuterium in the form of HD or D_2. Figure 1 shows the HD displacement transients for Ru, Rh, and Ni, measured at 298 K. The absisca in this, and subsequent figures, is expressed as the moles of HD formed per second divided by the moles of surface metal atoms, the latter quantity being determined by the mass of metal powder used and its dispersion. D_2 transients similar to the HD transients were also observed; however, they were smaller due to the high H_2 partial pressure. The shapes of the HD transient for each metal are similar, showing a single narrow peak with a width at half height of about 1 s.

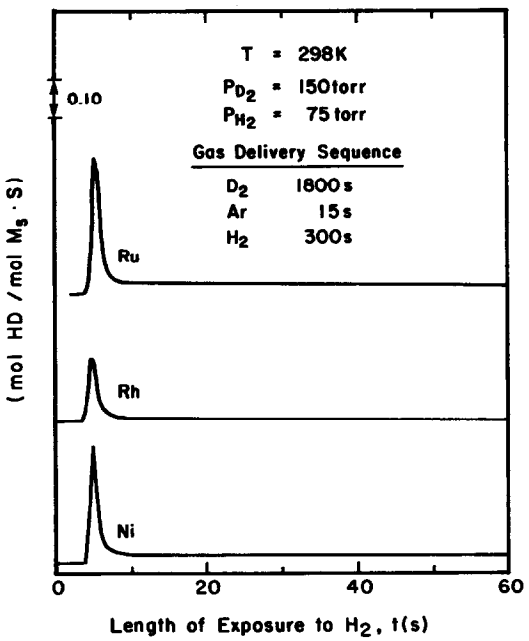

FIG. 1. Transient responses for weakly adsorbed deuterium. T_{ads} = 298 K.

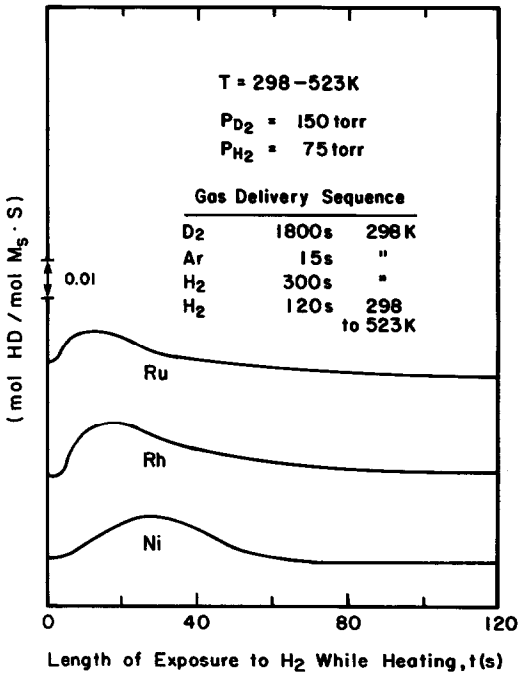

FIG. 2. Transient responses for weakly adsorbed deuterium observed while ramping the catalyst temperature from 298 to 523 K.

Following 300 s of exchange with H_2 at 298 K, the temperature was ramped to 523 K in approximately 120 s by submerging the reactor in a preheated sand bath. During this time, additional deuterium was displaced as HD, as shown in Fig. 2, but no D_2 was observed. The HD transients for each metal consist of a single broad peak. Physical significance cannot be attributed to differences in peak position due to the impre-

TABLE 2

Deuterium Coverages at 298 K Measured in the Presence and Absence of Coadsorbed CO

Metal	CO absent			CO present		
	θ_D^{LT}	θ_D^{HT}	θ_D^T	θ_D^{LT}	θ_D^{HT}	θ_D^T
Ru	0.71	0.41	1.12	0.06	0.23	0.29
Rh	0.68	0.53	1.20	0.0	0.54	0.54
Ni	0.98	0.64	1.62	0.04	0.57	0.61

Note. $T_{adsorption}$ = 298 K.

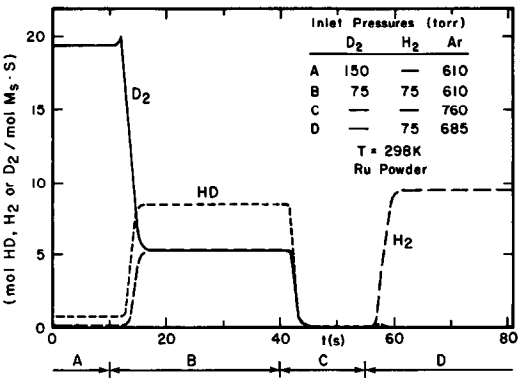

FIG. 3. Steady-state isotopic scrambling of H_2 and D_2 at 298 K.

cision of the temperature ramping and monitoring arrangement.

By integrating the transients shown in Figs. 1 and 2, one can determine the amount of deuterium adsorbed in low-energy states exchangeable at 298 K, designated as θ_D^{LT}, and that adsorbed in higher-energy states exchangeable at elevated temperatures, designated as θ_D^{HT}. Values of θ_D^{LT}, θ_D^{HT}, and the total deuterium coverage, designated as θ_D^T are given in Table 2. The ratio $\theta_D^{LT}/\theta_D^{HT}$ is about 1.5 for each of the metal powders studied. The total coverage by both forms of adsorbed deuterium exceeds unity and increases in the order Ru < Rh < Ni.

The length of time a sample was flushed in Ar strongly affected the distribution of the two forms of adsorbed deuterium. To establish this, deuterium was adsorbed on a clean sample at 298 K, then flushed with Ar for either 15 or 300 s. The adsorbed deuterium was then displaced with H_2 at 298 K to determine θ_D^{LT}, then the temperature was ramped to 523 K to determine θ_D^{HT}. The distribution of θ_D^{LT} and θ_D^{HT} for each metal is summarized as a function of the length of Ar flushing in Table 3. For Ru and Ni powder, the value of θ_D^{LT} declines substantially, while θ_D^{HT} falls only moderately, with increasing Ar flushing. Rh exhibits a different behavior; though θ_D^{LT} and θ_D^T decrease, θ_D^{HT} actually increases by 25%. Clearly, a conversion of the low-energy form to the high-energy form has occurred on the Rh powder during the flushing with Ar at 298 K.

TABLE 3

Effects of Ar Flushing Duration on the Surface Coverage of Adsorbed Deuterium

Metal	15 s Ar			300 s Ar		
	θ_D^{LT}	θ_D^{HT}	θ_D^T	θ_D^{LT}	θ_D^{HT}	θ_D^T
Ru	0.71	0.41	1.12	0.56	0.44	1.00
Rh	0.68	0.53	1.20	0.34	0.66	1.00
Ni	0.98	0.64	1.62	0.49	0.51	1.00

Note. $T_{adsorption}$ = 298 K.

Figure 3 illustrates the results of an experiment in which a ruthenium sample previously treated with D_2 for 1800 s at 298 K, was switched to a 50 : 50 mixture of $H_2 : D_2$. Scrambling of the $H_2 : D_2$ mixture resulted in HD formation within 93% of equilibrium. After 30 s, the reactor was flushed with Ar for 15 s, then the surface was exchanged with H_2. The resulting HD transient is shown in Fig. 4. For comparison, the HD transient which results from an identical sequence, but not including exposure to the $H_2 : D_2$ mixture, is also shown in Fig. 4. The value of θ_D^{LT} is reduced in half by exposure to the $H_2 : D_2$ mixture. Upon ramping the catalyst temperature to 523 K, the high-energy form of deuterium is displaced, producing the HD transient shown in Fig. 5.

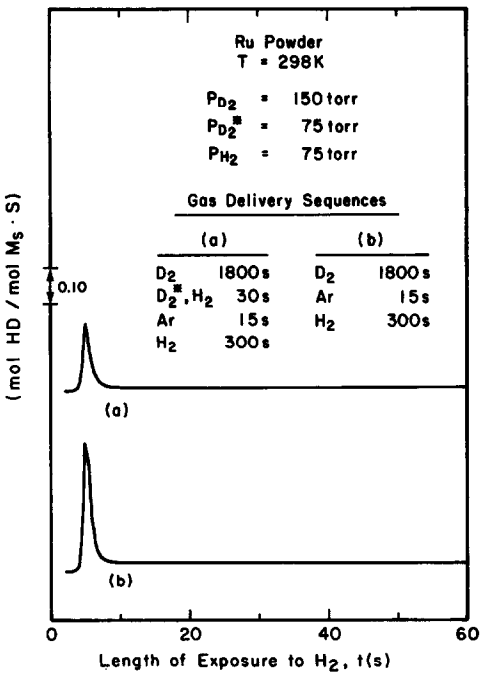

FIG. 4. Effect of catalyst exposure to a H_2–D_2 mixture at 298 K on the transient responses for weakly adsorbed deuterium. (a) Following 30-s exposure to 50:50 H_2–D_2 mixture. (b) Following exposure to D_2.

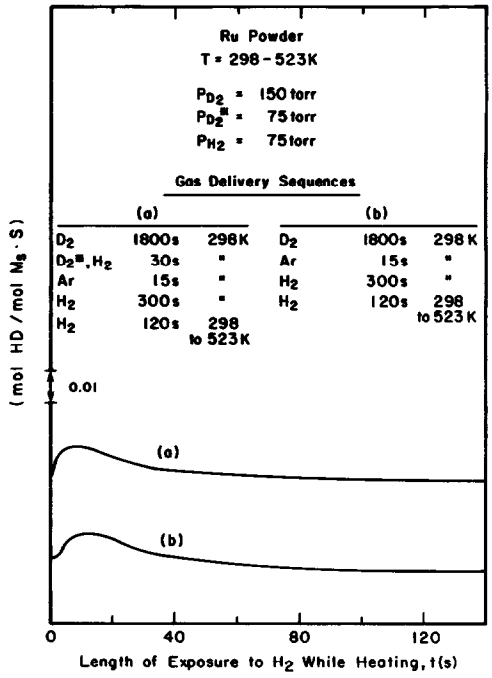

FIG. 5. Effect of catalyst exposure to a H_2–D_2 mixture at 298 K on the transient responses for strongly adsorbed deuterium. (a) Following 30-s exposure to 50:50 D_2–H_2 mixture. (b) Following exposure to D_2.

The high-temperature HD transient which results from a sequence not including exposure to the 50:50 H_2:D_2 mixture is also shown in Fig. 5. Both transients are of equivalent magnitude indicating that the high-energy form of adsorbed deuterium is not in equilibrium with the gas phase.

The presence of adsorbed CO has a significant influence on the amount of adsorbed deuterium and its exchange with the gas phase. The HD transient shown in Fig. 6 is obtained when a catalyst saturated with D_2 is exposed to a mixture of D_2 and CO for 300 s at 298 K, flushed with Ar for 15 s, then exposed to H_2. Very little deuterium is exchanged off the surface at 298 K in the presence of adsorbed CO, as can be seen by comparing Fig. 6 with Fig. 1. When the temperature is ramped to 523 K, HD is generated as shown in Fig. 7. The amounts of adsorbed deuterium present in low- and high-energy forms, with and without the presence of adsorbed CO are compared in

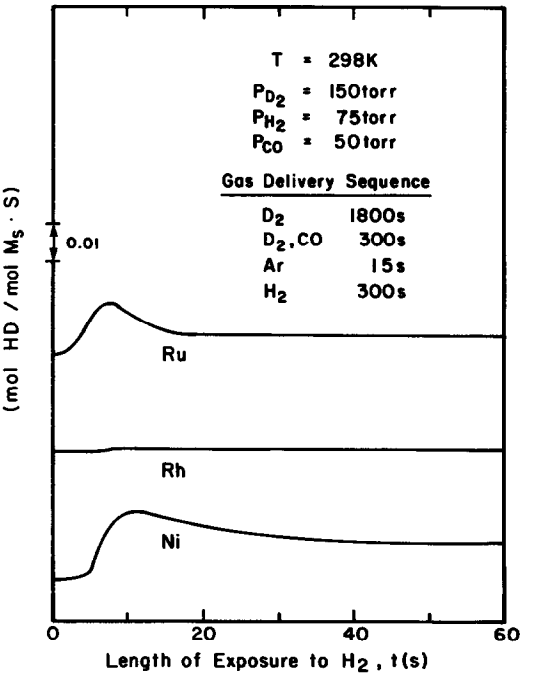

FIG. 6. Transient responses for weakly adsorbed deuterium following coadsorption of D_2 and CO at 298 K.

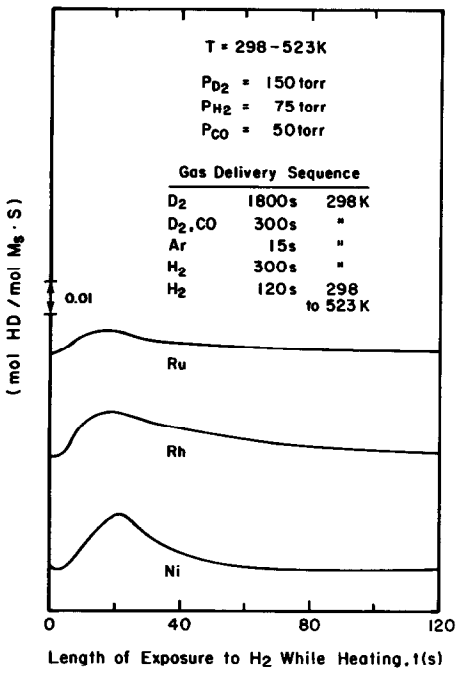

FIG. 7. Transient responses for strongly adsorbed deuterium following coadsorption of D_2 and CO at 298 K.

Table 2. Most of the weakly adsorbed deuterium is displaced by CO, while the strongly held form is essentially unaffected.

The presence of adsorbed CO completely inhibits isotopic scrambling of H_2 and D_2 at 298 K. This can be seen in Fig. 8, which illustrates the results of an experiment in which a ruthenium sample previously treated with D_2 and CO for 300 s is switched to a mixture of D_2, H_2, and CO. No H_2–D_2 scrambling is observed. After 30 s, the reactor is flushed with Ar for 15 s, then the surface is exchanged with H_2. The resulting transient is shown in Fig. 9. For comparison, the HD transient which results from an identical sequence, but excluding exposure to the $H_2 : D_2 : CO$ mixture is also shown in Fig. 9. Both transients are identical indicating that adsorbed CO inhibits exchange of the small amount of weakly adsorbed deuterium with H_2 and D_2 in the gas phase. Upon ramping the catalyst temperature to 523 K, the high-energy form of deuterium is displaced, producing the HD transient

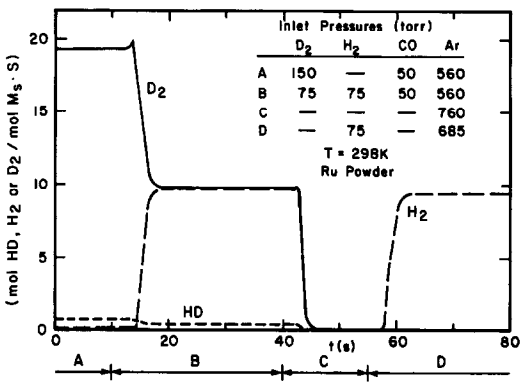

FIG. 8. Steady-state isotopic scrambling of H_2 and D_2 in the presence of CO at 298 K.

shown in Fig. 10. The high-energy HD transient which results from a sequence not including exposure to the $H_2 : D_2 : CO$ mixture exposure is shown in Fig. 10. The similarity of the two transients indicates that the amount of the high-energy form of adsorbed deuterium is unaffected by the exposure to the $H_2 : D_2 : CO$ mixture.

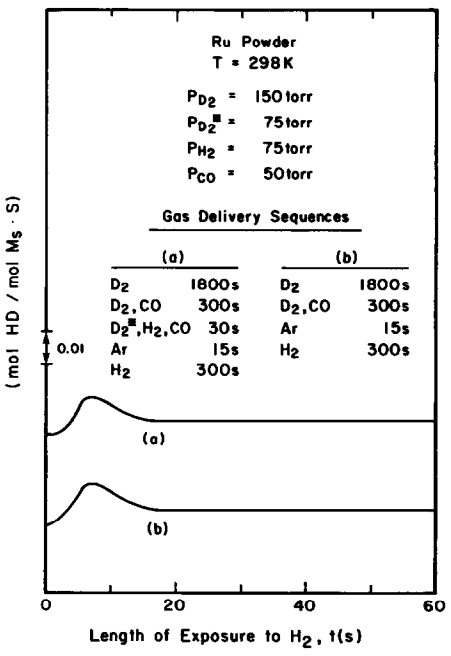

FIG. 9. Effect of catalyst exposure to an $H_2 : D_2 : CO$ mixture on the transient responses for weakly adsorbed deuterium. (a) Following 30-s exposure to 50 : 50 $D_2 : H_2$ with CO. (b) Following exposure to D_2 and CO.

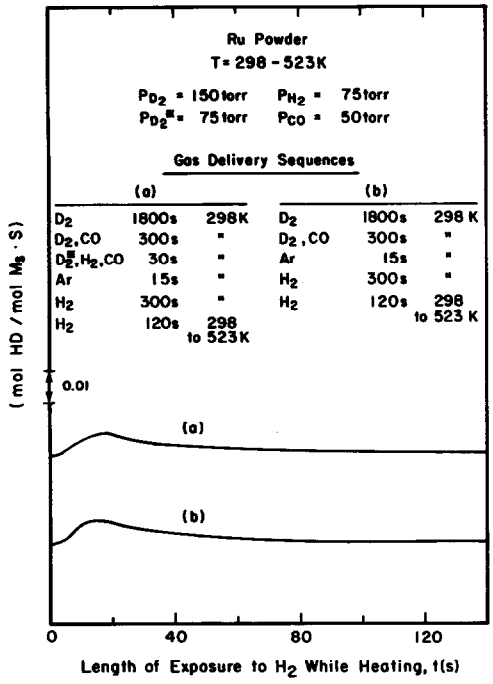

FIG. 10. Effect of catalyst exposure to an $H_2:D_2:CO$ mixture on the transient responses for strongly adsorbed deuterium. (a) Following 30-s exposure to 50 : 50 $D_2:H_2$ with CO. (b) Following exposure to D_2 and CO.

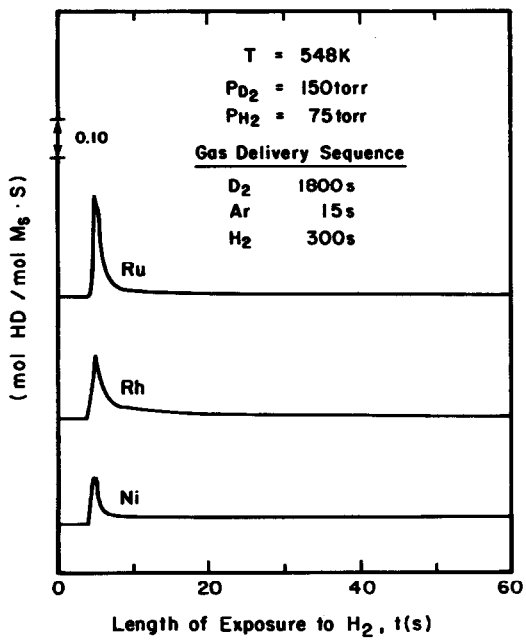

FIG. 11. Transient responses for adsorbed deuterium. T_{ads} = 523 K.

TABLE 4

Deuterium Coverages at 523 K Measured in the Presence and Absence of Coadsorbed CO

Metal	CO absent	CO present
	θ_D^T	θ_D^T
Ru	0.53	0.19
Rh	1.01	0.69
Ni	0.24	0.16

Note. $T_{adsorption}$ = 523 K.

The influence of temperature on the surface concentration of deuterium was also studied. When a sample at 523 K is exposed to D_2 for 1800 s, flushed with Ar for 15 s, then exposed to H_2, the HD transients in Fig. 11 are observed. At 523 K the transient cannot be decomposed into two components. The quantity of deuterium displaced from the surface of each catalyst is given in Table 4. Comparison of the data in Tables 2 and 4 indicates that the adsorption of deuterium at 523 K is significantly lower than at 298 K. The extent of the decrease changes in the order Ni > Ru > Rh.

The adsorption of deuterium at 523 K is further suppressed by the presence of CO, as demonstrated by the results summarized in Table 4. The inhibition of deuterium adsorption by CO at 523 K decreases in the order Ru > Ni > Rh. Comparison of Tables 2 and 4 reveals that the effects of increasing temperature on deuterium chemisorption in the presence of CO is not the same on all three metals. For Ru and Ni, θ_D^T is smaller at 523 K than at 298 K, but for Rh, the reverse is true.

Studies of H_2–D_2 scrambling carried out at 523 K demonstrated that CO does not inhibit scrambling at this temperature. It was also established that all forms of adsorbed deuterium are in equilibrium with the gas-phase composition at 523 K.

Adsorbed CO

The surface concentration of adsorbed CO was measured by isotopic displacement

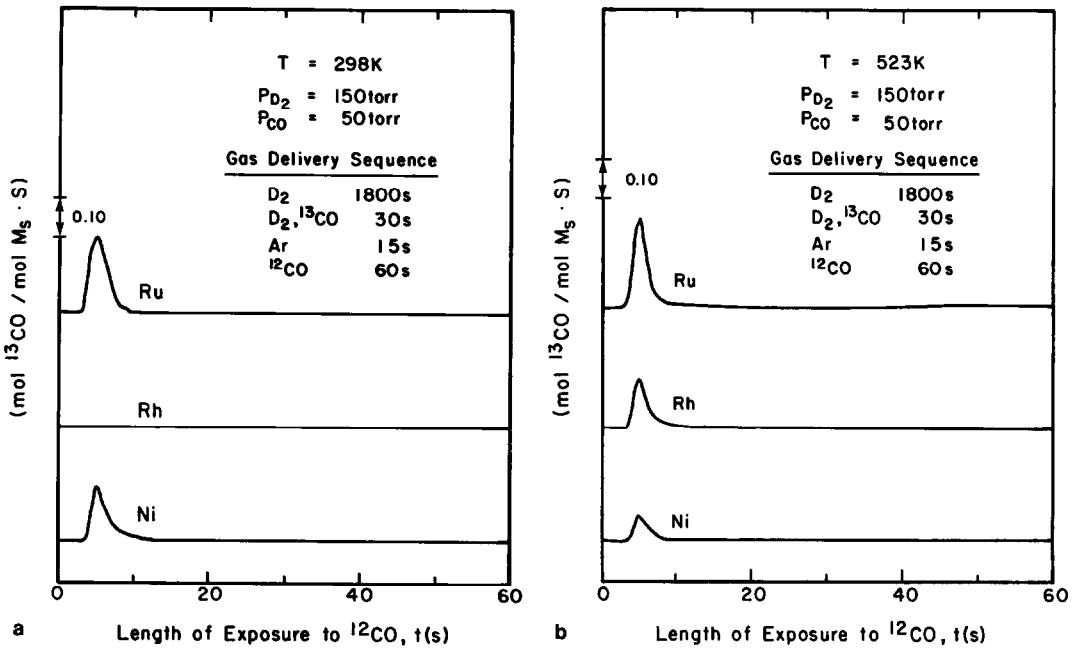

FIG. 12. (a) Transient response for adsorbed ^{13}CO. T_{ads} = 298 K. (b) Transient response for adsorbed ^{13}CO. T_{ads} = 523 K.

using the following procedure. A freshly reduced catalyst was exposed to a mixture of D_2 and ^{13}CO at the desired temperature for 30 s. The reactor was flushed with Ar for 15 s, then a stream of ^{12}CO was introduced. The ^{13}CO displaced by the adsorbing ^{12}CO resulted in a ^{13}CO transient.

The ^{13}CO transients observed at 298 and 523 K are shown in Figs. 12a and b. At 298 K, ^{12}CO quantitatively displaces adsorbed ^{13}CO from Ni and Ru, but only trace amounts from Rh (Fig. 12a). The ^{13}CO adsorbed on Rh at 298 K could be displaced when the temperature was ramped to 523 K in ^{12}CO. Due to the long broad nature of the ^{13}CO transient from Rh, no accurate estimate could be made of the CO : Rh_s ratio at 298 K. No additional ^{13}CO was displaced upon increasing the temperature of the Ni or Ru samples.

When ^{13}CO was adsorbed at 523 K, the ^{13}CO displacement transients in Fig. 12b were observed. The amounts of ^{13}CO displaced from each sample are summarized in Table 5. It is evident that the CO coverages for Ru measured at 298 and 523 K are comparable. For Ni, though, the CO coverage at 523 K is significantly lower than at 298 K.

Additional experiments were conducted to determine the influence of the presence or absence of adsorbed deuterium, and the length of exposure to ^{13}CO on the amount of adsorbed CO observed. Neither had a measurable effect on the CO coverage.

Adsorbed Carbon Species

The amounts and reactivities of adsorbed carbon species were determined using procedures similar to those described in Refs.

TABLE 5

Coverages of Adsorbed CO at 298 and 523 K

Metal	θ_{CO}(298 K)	θ_{CO}(523 K)
Ru	0.76	0.76
Rh	N.O.[a]	0.38
Ni	0.74	0.44

[a] Not observable because CO is displaced in a long broad transient at elevated temperatures.

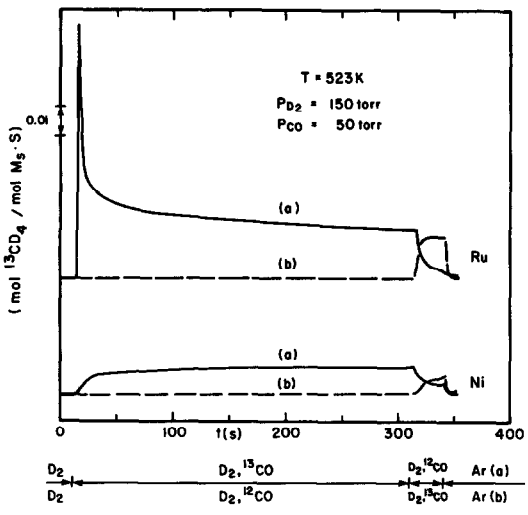

FIG. 13. The rate of $^{13}CD_4$ formation during the following sequences: (a) $D_2 \rightarrow D_2$, ^{13}CO (300 s) $\rightarrow D_2$, ^{12}CO (30 s) $\rightarrow$ Ar. (b) $D_2 \rightarrow D_2$, ^{12}CO (300 s) $\rightarrow D_2$, ^{13}CO (30 s) $\rightarrow$ Ar.

(*4–6*). In brief, following reduction of the catalyst in D_2 for 1800 s at the reaction temperature, a mixture of D_2 and ^{13}CO is fed to the reactor. The rate of $^{13}CD_4$ is then monitored until a quasisteady state is achieved. At the end of the reaction period, typically 300 s, the catalyst surface contains ^{13}C-labeled carbon and carbon monoxide. The adsorbed ^{13}CO is rapidly displaced by substituting a mixture of D_2 and ^{12}CO for the mixture of D_2 and ^{13}CO. During the time that ^{12}CO is present in the feed, the rate of $^{13}CD_4$ formation decreases monotonically, due primarily to the consumption of ^{13}C-labeled carbon. Since the logarithm of the rate of $^{13}CD_4$ formation versus time plots as a straight line, the kinetics can be described by

$$r_{^{13}CD_4} = \frac{d\theta_{^{13}C}}{dt} = -k\theta_{^{13}C}, \qquad (1)$$

where k is the apparent first-order rate coefficient and $\theta_{^{13}C}$ is the surface coverage by active carbon. Integration of Eq. (1) gives

$$\theta_{^{13}C} = \theta^{\circ}_{^{13}C} \exp(-kt), \qquad (2)$$

where $\theta^{\circ}_{^{13}C}$ is the initial coverage of active ^{13}C carbon prior to the introduction of ^{12}CO. From a fit of Eq. (2) to the experimental data, both k and $\theta^{\circ}_{^{13}C}$ can be determined.

At the end of the period of exposure to the catalyst to D_2 and ^{12}CO, the reactor is flushed with Ar and then D_2 is introduced to react off any residual ^{13}C carbon and adsorbed ^{12}CO. Integration of the transients produced during this period gives the quantity of residual carbon on the catalyst and the coverage by adsorbed CO (*4–6*).

The rate of $^{13}CD_4$ formation during the first 300 s of exposure to D_2 and ^{13}CO are shown in Fig. 13 for Ru and Ni. The rate of methane formation over Rh was too small to measure accurately for the conditions indicated. The relative order of activities for the three catalysts (i.e., Ru > Ni $\gg$ Rh) is in agreement with previous observations (*17*). For Ru and Ni, the rates of formation of CO_2 and C_2^+ hydrocarbons were always less than 10% of the methane formation rate.

Following 300 s of reaction, the feed was switched from D_2 and ^{13}CO, to D_2 and ^{12}CO. Since the adsorbed ^{13}CO is rapidly displaced by ^{12}CO, the $^{13}CD_4$ produced after the exchange of CO isotopes (see Fig. 13) is generated from the reduction of ^{13}C-labeled carbon species (*4–6*). The transients observed when the order of introduction of CO isotopes is reversed are also shown in Fig. 13. An increase in $^{13}CD_4$ formation is now observed following the substitution of ^{12}CO by ^{13}CO in the feed mixture, as ^{13}C is incorporated into the carbon pool. The surface concentration of active carbon and the apparent first-order rate coefficient for ^{13}C-carbon consumption were determined by fitting Eq. (2) to the experimental data. Values of $\theta^{\circ}_{^{13}C}$, hereafter designated θ_C, and k are given in Table 6. Due to the low activity of Rh, no estimate of θ_C or k was possible for this catalyst.

After 30 s of exchange, the reactor was flushed with Ar for 15 s, and the catalyst was then reduced in D_2. The $^{13}CD_4$ transients shown in Fig. 14 were obtained during catalyst reduction. The transients observed following exchange with D_2 and

TABLE 6

Coverages of Carbon and Carbon Monoxide Measured under Reaction Conditions at 523 K

Metal	Via exchange		Via reduction	
	θ_C	k (s^{-1})	θ_C	θ_{CO}
Ru	~0.12	0.10	0.23	0.74
Rh	N.O.[a]	N.O.[a]	~0.01	N.O.[a]
Ni	~0.25	0.05	0.71[b]	0.37

[a] Not observable.
[b] Active carbon ~0.15. Inactive carbon ~0.55.

^{12}CO are referred to as a $^{13}CD_4/C_s$ transients since they result from reducing ^{13}C-labeled carbonaceous species from the surface. There is no contribution due to the adsorbed CO since all the adsorbed ^{13}CO has been displaced from the surface by ^{12}CO. The transients observed following exchange with D_2 and ^{13}CO are referred to as $^{13}CD_4/CO_s$ transients since they result primarily from reducing adsorbed CO from the surface. These transients also include a small contribution from ^{13}C-labeled carbon species that are generated during the exchange. A summary of the coverages calculated from the $^{13}CD_4/C_s$ and $^{13}CD_4/CO_s$ transients is given in Table 6 for each metal powder.

The results for Ru agree favorably with those reported previously (*6*). Fitting the decline in the rate of methanation during exchange to first-order kinetics gives an estimate of $\theta_C = 0.12$. The $^{13}CD_4/CO_s$ transient yields an estimate of $\theta_{CO} = 0.74$, in good agreement with the value of $\theta_{CO} = 0.76$ from CO isotope exchange results in Table 5. However, since the exchange went to near completion, the $^{13}CD_4/CO_s$ transient includes a contribution of about 0.1 monolayer equivalents from adsorbed carbon. Integration of the $^{13}CD_4/C_s$ transient gives $\theta_C = 0.23$. Since exchange has gone to near completion, this carbon must result from a surface residue similar to the C_β reported in Refs. (*5, 6*).

Only a small, slow $^{13}CD_4/C_s$ transient, corresponding to a surface coverage of about 0.01 monolayer equivalents of adsorbed carbon, was observed on Rh. No $^{13}CD_4/CO_s$ transient was observed indicating that even in the presence of pure H_2, the CO adsorbed on Rh does not react at 523 K. The low surface concentrations of adsorbed active carbon, and the lack of reduction of adsorbed CO to methane contribute to the extremely low methanation activity of the Rh powder.

For Ni powder, reduction gives an estimated $\theta_{CO} = 0.37$. This is in good agreement with the value of 0.44 given in Table 5, which is determined by isotopic displacement of CO at 523 K. The value of θ_{CO} determined via reduction, however, includes a contribution due to ^{13}C incorporation during exchange of about 0.1 monolayer equivalents. Modeling the change in $^{13}CD_4$ formation during steady-state CO exchange yielded an estimate of $\theta_C = 0.25$, however titration gives $\theta_C = 0.71$. This discrepancy

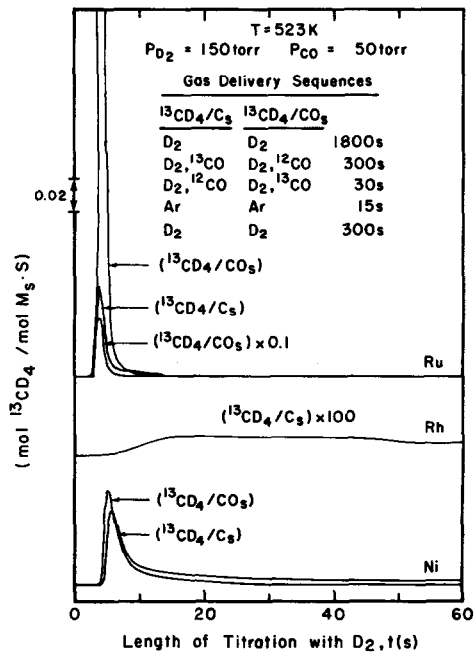

FIG. 14. Transient responses observed during the reduction of the catalyst with D_2 following the reaction conditions indicated in Fig. 13.

is due to the long tail in the $^{13}CD_4/C_s$ transient shown in Fig. 14. This tail results from reduction of an inactive carbon species. By subtracting out the tail of the transient, it is possible to estimate the amount of active carbon on the catalyst surfaces. This corresponds to about 0.15 monolayer equivalents, in reasonable agreement with the exchange results. The amount of inactive carbide corresponds to a surface concentration of about 0.55 monolayer equivalents.

DISCUSSION

Adsorbed Deuterium

Experiments carried out in this study clearly demonstrate the presence of two forms of adsorbed hydrogen. The first is a low-energy form which at 298 K is in isotopic equilibrium with the gas phase and is largely displaced by adsorbing CO. The second is a high-energy form which at 298 K is not in isotopic equilibrium with the gas phase and is not displaced by adsorbing CO. To explain the origins of these two forms of adsorbed hydrogen, it is useful to review the available information concerning H_2 adsorption on single-crystal surfaces, polycrystalline powders, and supported crystallites of Group VIII metals.

Temperature-programmed desorption studies carried out with single-crystal surfaces of Group VIII metals typically show a single desorption maximum for H_2 (*18–36*). Moreover, investigations of smooth and stepped surfaces of Rh (*31*), Ni (*32, 33*), and Ru (*24*) have shown that the desorption behavior of H_2 is fairly independent of surface topology. While EELS studies (*37*) have suggested that there may be two adsorption sites for H_2 on Ru (001), the energy difference between these two sites is small since substitution of D_2 for H_2 leads to complete displacement. It has also been found that CO adsorption on single crystal surfaces blocks the adsorption of H_2 at temperatures above 300 K (*18–23, 34–36*).

In contrast to the behavior of single-crystal surfaces, temperature-programmed desorption of H_2 from polycrystalline powders and supported crystallites of Group VIII metals often exhibit multiple desorption peaks (*38–45*). In the case of H_2 desorption from Rh/SiO_2 (*44*), analysis of the TPD spectra leads to estimates of the activation energies for desorption of 14 and 21 kcal/mol, but the nature of the two adsorption sites is not identified. Only a very limited amount of information is available about the interactions of adsorbed H_2 with D_2 or CO for polycrystalline samples. H_2–D_2 exchange experiments conducted with Pt, Rh, and Ir filaments have shown that preadsorbed H_2 is replaced by D_2 from the gas phase, and that coadsorbed mixtures of H_2 and D_2 result in equilibrium isotopic mixing upon desorption (*38, 46*). Similar experiments are usually not performed with supported metals because of problems associated with H_2–D_2 exchange with the support. Complete displacement of H_2 preadsorbed on Pd/SiO_2 has been reported though (*47*).

From the preceding discussion it is evident that the low-energy form of adsorbed hydrogen observed here exhibits characteristics identical to those for H_2 adsorbed on single-crystal surfaces. The high energy form is more difficult to interpret. While high-temperature states of adsorbed H_2 are observed for Group VIII metal powders and supported crystallites, their origins remain unexplained. One possibility is that they occur at defects or contamination sites. Another, and perhaps more plausible, explanation is that the high-energy forms of adsorbed H_2 correspond to hydrogen which has migrated into the bulk of the larger powder particles by diffusion along crystallite grain boundaries. This interpretation would explain why the high-energy form does not undergo H_2–D_2 exchange at 298 K or displacement by CO. The proposed interpretation is also consistent with the observation of an increase in the coverage of H_s^{HT} during Ar purging at 298 K over Rh (see Table 3) and the more facile exchange between H_s^{LT} and H_s^{HT} at high temperature.

Finally, if only H_s^{HT} is regarded as hydrogen adsorbed on the exterior surfaces of metal particles, then comparison of Tables 3 and 5 demonstrates that the stoichiometry for surface adsorbed H and CO are in reasonable agreement.

Adsorbed Carbon Monoxide

Similarities were observed in the absorption of CO on Ru and Ni powders. For both metals the saturation coverage at 298 K was approximately 0.75 (see Table 5) and complete isotopic exchange occurred at this temperature. The saturation coverage observed for Ru powder in the present study is less than that reported recently by Winslow and Bell (θ_{CO} = 0.85–1.0) (*6*). On the other hand, the saturation coverage observed here for Ni powder is greater than that reported by Bartholomew and Pannell (θ_{CO} = 0.55) (*48*). The discrepancies may be due to differences in the sources and purities of the metal powders and the techniques used to define a monolayer. Thus, for example, if the coverage by H_s^{LT} following a 15-s Ar purge is used to define monolayer coverage, the CO coverage for Ru would be close to unity and that for Ni would be 0.45.

The behavior of Rh with respect to CO chemisorption was significantly different from that of Ru and Ni. At 298 K, the adsorbed CO did not undergo isotopic displacement. Only by ramping the temperature could the CO be displaced from the Rh surface. This behavior is suggestive of an activated CO exchange process. The reasons for the greater difficulty in isotopic substitution of CO adsorbed on Rh compared to Ru or Ni, is not apparent. While, as shown in Table 7, the activation energy for CO desorption from Rh single-crystal surfaces is higher than that for desorption from Ni surfaces, it is comparable to that for Ru surfaces.

TABLE 7

Activation Energies for CO Desorption from Single-Crystal Surfaces of Ru, Rh, and Ni

Surface	E_d[a] (kcal/mol)	Reference
Ru(001)	28.2	(*7*)
Ru(001)	30.0	(*22*)
Ru(110)	29	(*15*)
Rh(100)	30.5	(*13*)
Rh(111)	31.6	(*20*)
Rh(110)	31.1	(*21*)
Ni(100)	27.1	(*12*)
Ni(100)	27.6	(*10*)
Ni(111)	26.4	(*9*)
Ni(111)	26	(*19*)

[a] Based on Redhead analysis (*51*) at saturation coverage for highest-energy desorption peak, assuming $k_d = 10^{13}$ s^{-1}.

Adsorbed Carbon

Adsorbed carbon was observed on each of the metal powders following the hydrogenation of CO. On Rh powder, however, only traces of carbon could be reduced off the surface at 523 K. Solymosi *et al.* (*10*) observed carbon accumulations on various supported Rh catalysts. For Rh/SiO_2 the carbon accumulation after 60 min of reaction at 523 K was 0.11 monolayer equivalents. However, 90% of this carbon required temperatures of 623 K and above to be removed. Rh/Al_2O_3 and Rh/TiO_2 were more active for methanation and accumulated larger quantities of carbon. Again, temperatures in excess of 623 K were required to remove 85% of the carbon on Rh/Al_2O_3 and 96% of the carbon on Rh/TiO_2. These studies suggest that the reduction of Rh powder at 523 K may have been insufficient to remove all of the adsorbed carbon species. The results on Rh powder, however, clearly show that active carbon species are present at very low surface coverages in comparison to the Ru and Ni powders.

Considerable amounts of carbon accumulate on the surfaces of Ni and Ru during methanation. Only a portion of the total carbon pool, though, is active carbon directly involved in methanation. The amounts observed were about 0.12 mono-

layer equivalents for Ru and about 0.25 monolayer equivalents for Ni. Previous studies on Ru/SiO_2 and Ru powder have demonstrated that the rate of methanation is directly proportional to the surface concentration of this form of carbon (*5, 6*).

Carbon deposits which are less active with respect to hydrogenation were also observed on Ru and Ni. On Ru, 0.23 monolayer equivalents of such "less active" carbon was observed at 523 K. This carbon form is similar to the "less active" carbon form reported in our earlier work on Ru powder, which was designated as C_β (*6*). This C_β carbon form was present at 0.7 monolayer equivalents at 443 to 463 K. It is possible that the reason for the lower surface concentration of adsorbed carbon on Ru at 523 K is its more rapid removal at this temperature than at lower temperatures. If this interpretation is correct, it would imply that the activation energy for hydrogenation of the "less active" carbon is greater than the activation energy for its formation. An alternative explanation is that at higher temperatures, a larger proportation of the carbon pool is converted to a form of carbon which does not undergo hydrogenation at the reaction temperature. Indeed, NMR studies (*11*) have demonstrated that extended low temperature reduction of used Ru/SiO_2 methanation catalysts leaves a graphite-like carbon deposit remaining on the catalyst hours after reduction.

Carbon deposits were also observed on Ni powder by reduction with deuterium. For Ni, however, the titration transient was deconvoluted into two portions. The initial sharp peak with surface concentration of about 0.15 monolayer equivalents is associated, at least in part, with the active carbon observed during CO exchange. The active carbide is observable on Ni powder during titration since during the CO exchange the labeled methane rate only declined by about 60%, leaving behind part of the active carbon remaining on the surface to be removed during titration. This is to be compared with the results for Ru powder, where only the "less active" carbon was observable during reduction. Since the rate of formation of $^{13}CD_4$ on Ru decreased by 90% during CO exchange, very little of the active carbon is left on the surface to be removed during titration. An additional inactive carbon species is observed on Ni as exhibited by the long tail in the reduction transient shown in Fig. 13.

The concentrations of adsorbed carbon species observed on Ni powder are in line with the range of 0.05 to 0.50 monolayer equivalents observed by Kelley and Semancik (*49*) on a Ni (100) surface at 625 K. More recently, Yang *et al.* (*50*) have measured the surface accumulations of carbon on Ni catalysts, using techniques similar to those used in the present study. At 523 K, these authors reported $\theta_C = 0.05$ for Ni/SO_2 and $\theta_C = 0.4$ for Raney Ni. The apparent first-order rate coefficient for carbon consumption was 0.03 s^{-1} at 513 K, which agrees closely with the value of 0.05 s^{-1} at 523 K reported here (see Table 6).

It is apparent from the present study that methanation activity is closely related to the presence of active carbon species on the catalyst surface. On both Ni and Ru, significant coverages of active carbon were observable via isotope exchange and reduction procedures. These catalysts were also active in methanation. Rh powder, in contrast, was deficient in the presence of active carbon species, and was also inactive for methanation. In addition what little carbon was observed on Rh, reacted very slowly with hydrogen. The requirement of an active carbon species agrees with earlier work on Ru/SiO_2 and Ru powder which demonstrated that the methanation activity is directly proportional to the surface concentration of the most active surface carbon species, designated as C_α (*5, 6*).

The conversion of adsorbed carbon to methane requires the participation of adsorbed hydrogen (deuterium). The present investigation demonstrates that the surface concentration of adsorbed hydrogen is significant under reaction conditions and

hence the availability of this species does not appear to limit the rate of reaction. In this connection, it is significant that the values of θ_D is larger for Rh than for either Ru or Ni. This observation further supports the contention that what limits the rate of methanation on Rh is the rate CO dissociation to form carbon and the intrinsically low reactivity of what carbon is formed. While it has been observed that the rate of methane formation is first order in the surface coverage of active carbon, the dependence on the coverage of hydrogen is not known and requires further study.

CONCLUSIONS

Two forms of adsorbed hydrogen are observed on Ru, Rh, and Ni powders at 298 K. The weakly adsorbed form is in equilibrium with the gas phase and is rapidly displaced by the adsorption of CO. The behavior of this form of adsorbed hydrogen is quite similar to that observed on clean metal surfaces. The strongly adsorbed form does not participate in H_2–D_2 exchange at 298 K nor is it displaced by CO at 298 K. This form of adsorbed hydrogen may be hydrogen which has migrated into the interior of the metal particles by diffusion along crystal grain boundaries. Carbon and CO are also present on the catalyst surface during CO hydrogenation. Adsorbed ^{13}CO is rapidly displaced by ^{12}CO at 298 and 523 K on Ru and Ni. For Rh, temperatures above 298 K are required for isotopic displacement of adsorbed CO. Active carbon species are observable on the Ru and Ni powders, but no on Rh. It is shown that high methanation activity correlates with surface coverage of active carbon and not with the coverage of adsorped hydrogen.

ACKNOWLEDGMENTS

This work was supported by the Division of Chemical Sciences, Office of Basic Energy Sciences, U.S. Department of Energy, under Grant DE-AC03-76SF0098.

REFERENCES

1. Rabo, J. A., Risch, A. P., and Poutsma, W. M. H., *J. Catal.* **53,** 295 (1978).
2. Biloen, P., Helle, J. N., and Sachtler, W. M. H., *J. Catal.* **58,** 95 (1979).
3. Sachtler, J. W. A., Kool, J. M., and Ponec, V., *J. Catal.* **84,** 358 (1983).
4. Cant, N. W., and Bell, A. T., *J. Catal.* **73,** 257 (1982).
5. Winslow, P., and Bell, A. T., *J. Catal.* **86,** 158 (1984).
6. Winslow, P., and Bell, A. T., *J. Catal.* **91,** 142 (1985).
7. Underwood, R. P., and Bennett, C. O., *J. Catal.* **86,** 245 (1984).
8. Bianchi, D., Tau, L. M., Borcar, S., and Bennett, C. O., *J. Catal.* **84,** 358 (1983).
9. Bianchi, D., Borcar, S., Teule-Gay, F., and Bennett, C. O., *J. Catal.* **84,** 442 (1983).
10. Solymosi, F., Tombacz, I., and Kocsis, M., *J. Catal.* **75,** 78 (1983).
11. Duncan, T. M., Winslow, P., and Bell, A. T., *Chem. Phys. Lett.* **102**(2,3), 163 (1983).
12. Vlasenko, V. M., Kukhar, L. A., Rusov, M. T., and Samchenko, N. P., *Kinet. Katal.* **5,** 337 (1964).
13. McKee, D. W., *J. Catal.* **8,** 240 (1967).
14. Kobori, Y., Yamasaki, H., Naito, S., Onishi, T., and Tamaru, K., *J. Chem. Soc., Faraday Trans. 1,* **78,** 1473 (1982).
15. Dalla Betta, R. A., *J. Catal.* **34,** 57 (1974).
16. Goodwin, J. G., *J. Catal.* **68,** 227 (1981).
17. Vannice, M. A., *J. Catal.* **37,** 462 (1975).
18. Peebles, D. E., Creighton, J. R., Belton, D. N., and White, J. M., *J. Catal.* **80,** 482 (1983).
19. Goodman, D. W., Yates, J. T., and Madey, T. E., *Surf. Sci.* **93,** L135 (1980).
20. Koel, B. E., Peebles, D. E., and White, J. M., *Surf. Sci.* **107,** L367 (1981).
21. Koel, B. E., Peebles, D. E., and White, J. M., *Surf. Sci.* **125,** 709 (1983).
22. Kim, Y., Peebles, H. C., and White, J. M., *Surf. Sci.* **114,** 363 (1982).
23. Peebles, D. E., Peebles, H. C., and White, J. M., *Surf. Sci.* **136,** 463 (1984).
24. Goodman, D. W., Madey, T. E., Ono, M., and Yates, J. T., *J. Catal.* **50,** 279 (1977).
25. Wedler, G., Papp, H., and Schroll, G., *J. Catal.* **38,** 153 (1975).
26. Kiskinova, M. P., and Bliznakov, G. M., *Surf. Sci.* **123,** 61 (1982).
27. Kok, G. A., Noordermeer, A., and Nieuwenhuys, B. E., *Surf. Sci.* **135,** 65 (1983).
28. Craig, J. H., *Surf. Sci.* **111,** L695 (1981).
29. Benziger, J. B., and Madix, R. J., *Surf. Sci.* **115,** 279 (1982).
30. Kawasaki, K., Shibata, M., Miki, H., and Kiuka, T., *Surf. Sci.* **81,** 370 (1979).
31. Castner, D. G., and Somorjai, G. A., *Surf. Sci.* **83,** 60 (1979).
32. Christman, K., Schober, O., Ertl, G., and Neumann, M., *J. Chem. Phys.* **60**(11), 4528 (1974).

33. Lapujoulade, J., and Neil, K. S., *J. Chim. Phys.* **70,** 797 (1973).
34. White, J. M., *J. Phys. Chem.* **87,** 915 (1983).
35. Peebles, D. E., Schreifels, J. A., and White, J. M., *Surf. Sci.* **116,** 117 (1982).
36. Williams, E. D., Thiel, P. E., Weinberg, W. H., and Yates, J. T., *J. Chem. Phys.* **72,** 3496 (1982).
37. Barteau, M. A., Broughton, J. Q., and Menzel, D., *Surf. Sci.* **133,** 443 (1983).
38. Popova, N. M., and Bebenkova, L. V., *React. Kinet. Catal. Lett.* **11,** 187 (1979).
39. Weatherbee, G. D., and Bartholomew, C. H., *J. Catal.* **79,** 196 (1983).
40. Uchida, M., and Bell, A. T., *J. Catal.* **60,** 204 (1979).
41. Jozwiak, K. W., and Paryjczak, T., *J. Catal.* **79,** 196 (1983).
42. Escard, J., LeClere, D., and Contour, J. P., *J. Catal.* **29,** 31 (1973).
43. Tsuchiya, S., Amenomiya, Y., and Cventanovic, R. J., *J. Catal.* **19,** 245 (1970).
44. Chin, A. C., and Bell, A. T., *J. Phys. Chem.* **87,** 3482 (1983).
45. Beck, D. D., Bawagan, A. O., and White, J. M., *J. Phys. Chem.* **88,** 2771 (1981).
46. Mimeault, V. J., and Hansen, R. S., *J. Chem. Phys.* **45,** 2240 (1966).
47. Rieck, J. S., and Bell, A. T., *J. Catal.*, in press.
48. Bartholomew, C. H., and Pannell, R. B., *J. Catal.* **65,** 390 (1980).
49. Kelley, R. D., and Semancik, S., *J. Catal.* **84,** 248 (1983).
50. Yang, C. H., Soong, Y., and Biloen, P., "Proceedings, 8th International Congress on Catalysis," Vol. II, p. 3. Verlag Chemie, Berlin, 1984.
51. Redhead, P. A., *Vacuum* **12,** 203 (1962).